China Geology 8 (2025) 754−764

China Geology

Journal homepage: http://chinageology.cgs.cn
https://www.sciencedirect.com/journal/china-geology

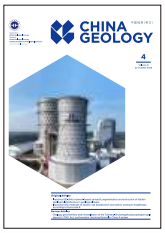

Spatial and temporal variations in parameters at the upper boundary of gas hydrate stability zone of the Sea of Okhotsk

Renat Shakirov[a], Vladimir Luchin[a], Evgeniya Petrova[a,*], Neng-you Wu[b], Yi-zhao Wan[b,*]

[a] *V.I. Il'ichev Pacific Oceanological Institute, Far Eastern Branch of the Russian Academy of Sciences (POI FEB RAS), Vladivostok* 690041, *Russia*
[b] *Qingdao Institute of Marine Geology, China Geological Survey, Qingdao* 266237, *China*

ARTICLE INFO

Article history:
Received 28 May 2024
Received in revised form 14 November 2024
Accepted 27 November 2024
Available online 13 December 2024

Keywords:
Methane hydrates
Thermobaric conditions
Stability zone
Upper boundary
Water column
Spatiotemporal variability
Sea of Okhotsk

ABSTRACT

This study was used oceanographic database in the Sea of Okhotsk between the period from 1929 to 2020 (131286 stations). The paper used gas hydrate dissociation parameters for the "pure methane-seawater" system obtained in the study by Dickens GR and Quinby-Hunt MS. The results have elucidated the spatiotemporal variability of distribution of such parameters at the upper boundary of the gas hydrate stability zone (GHSZ) as water temperature, salinity, and top depth of the stability zone. As the study has shown (based on average long-term spatial distributions), the minimum temperature and depth values of the GHSZ upper boundary in the Sea of Okhotsk occur off the western and southwestern parts of the water area. The maximum temperature and depth values of the GHSZ upper boundary are typical of the southeastern sea area and over the Kamchatka Peninsula slope. This study has also identified an area, where there are no thermobaric conditions for the emergence and stable existence of methane hydrates in the water column. The results presented agree well with the materials of observations conducted during expeditions and the previous data of predictive simulations for the Sea of Okhotsk.

1. Introduction

Gas hydrates (GH) are low-molecular-weight crystalline compounds formed under certain thermobaric conditions from water and gas. In GHs, gas molecules are enclosed in crystalline cells consisting of water molecules held together by a hydrogen bond. As pressure decreases or temperature increases, the hydrogen bond easily breaks down. In addition to thermobaric conditions, there are also other important factors responsible for GH formation, e.g., lithological ones such as the presence of porous and permeable sedimentary rocks (Istomin VA and Yakushev VS, 1992; Makogon YF, 2003, 2010; Reagan MT et al., 2011). According to recent estimates, about 99% of GH are concentrated on the continental shelf (Bondur VG et al, 2022).

Most of identified GH deposits have been found in seafloor sediments characterized by high porosity, low temperature, and unlithified host rocks. Permeability (k) of seafloor sediments varies significantly depending on sediment type. At low k values, no gases are released from sediments into seawater. Significant gas seeps (plumes) are formed at k values greater than 10^{-15} m^2 (or 1 mD) (Reagan MT et al., 2011).

GHs are compounds variable in composition. Besides individual hydrates, double and mixed hydrates (including several gases) are also known (Istomin VA and Yakushev VS, 1992). The origin of gases (within hydrates) is both thermogenic and biogenic. The gas component of biogenic origin consists almost entirely of methane (Chen ZA et al., 2005, 2010). In the gas components of thermogenic origin, in addition to methane, other gases are also present such as ethane, propane, etc. Known GH deposits usually consist of methane and small amounts of other gases (ethane, propane, carbon dioxide, etc.). For example, according to (Veselov OV et al., 2006), the gas composition of hydrates sampled in the Sea of Okhotsk: The methane content was 97.80%, the ethane content was 0.04%, and the carbon dioxide content was 0.09%. Presence of even a small percentage of gaseous methane homologues causes the phase boundary shift to

First author: *E-mail address*: ren@poi.dvo.ru (Renat Shakirov).

* Corresponding author: *E-mail address*: petrova@poi.dvo.ru (Evgeniya Petrova); wanyizhao@mail.cgs.gov.cn (Yi-zhao Wan).

Literary editor: Xi-jie Chen
doi:10.31035/cg2024087
2096-5192/© 2025 China Geology Editorial Office.

higher temperatures. The presence of propane in the gas mixture, compared to other gases, has a maximum effect on the equilibrium temperature (Holder GD et al., 1987; Sloan ED 1998; Sloan ED and Koh CA, 2008; Chen ZA et al., 2010; Giustiniani M et al., 2013).

In addition to the study of natural GHs as a potential resource of hydrocarbon raw materials, the study of their deposition areas is of major importance to address various environmental and climate change issues. With an increase in the near-bottom temperature, the thickness of GHSZ decreases, which can cause GHs to dissociate and methane to emit (Dickens GR and Quinby-Hunt MS, 1994; Reagan MT et al., 2011; Giustiniani M et al., 2013; Bogoyavlensky VI et al., 2018b). The gas released through hydrate decomposition (1 m^3 of GH yields about 160 m^3 methane (Makogon YF, 2003, 2010; Obzhirov AI and Shakirov RB, 2013; Yakutseni VP, 2013; Bondur VG et al, 2022) enters near-bottom waters. Then it enters into the atmosphere via currents, diffusion, and bubble transfer (Eliseev AV, 2018; Bondur VG et al, 2022). Since methane is an influential greenhouse gas (with the radiative forcing effect of CH_4 approximately 28–34-fold greater than that of CO_2 (Bondur VG et al, 2022), its entry into the atmosphere can cause serious climatic alterations (Biastoch A et al., 2011; Reagan MT et al., 2011; Smyshlyaev SP et al., 2015; Bogoyavlensky VI et al., 2018a, 2018b). The above facts, however, refer to shallow GH deposits, because a simulation of deep-sea hydrates (deeper than 1,000 m from the sea surface) has shown their relative insensitivity to changes in ocean temperature on a short time scale (Reagan MT and Moridis GJ, 2007; Giustiniani M et al., 2013).

The gas hydrate stability zone (GHSZ) is part of the Earth's lithosphere and hydrosphere whose thermobaric and lithological/geochemical regime fits the conditions for stable existence of hydrates of natural gases with certain compositions. GHSZs in the world's oceans tend to waters with depths greater than 200 m (for circumpolar regions) and 500–700 m (for equatorial regions). The upper boundary of the GHSZ is located, as a rule, in the water column and the lower one in seafloor sediments (Trofimuk AA et al., 1973; Makogon YF, 2003, 2010; Bogoyavlensky VI et al., 2018b).

Knowledge of the GHSZ top depth is required for:

(i) Modeling the dynamics of dissolution of ascending gas bubbles in the water column (McGinnis DF et al., 2006; Granin NG et al., 2010);

(ii) Modeling of GH responses to water temperature variations and for assessing the probability of methane emission into the ecosystem (with such important conditions as the positions of the boundaries and the GHSZ extent) (Biastoch A et al., 2011; Reagan MT et al., 2011; Giustiniani M et al., 2013);

(iii) Assessing the sensitivity of GHs to variations in external environmental factors (their dissociation and formation depending on the distance between the GHSZ top depth and the seafloor) (Reagan MT et al., 2007);

(iv) Planning surveys to find and study GHs in marine waters (Obzhirov AI and Shakirov RB, 2012, 2013; Jin YK et al., 2013, 2015; Shoji H et al., 2014; Minami H et al., 2016; Obzhirov AI, 2018);

(v) Describing gas "plumes" (seeps) (differentiated between shallow-water and deep-water plumes; deep-water gas flares are those located below GHSZ; flares above this water depth are defined as shallow-water gas seeps) (Granin NG et al., 2010).

To date, there is no information about spatiotemporal variations in the parameters at the GHSZ top depth of the Sea of Okhotsk. Bogoyavlensky VI with co-authors (2018a) have created the cartographic schemes of GHs and near-bottom water temperatures distribution in the Arctic and the World Ocean (on the basis of the summarizing database GIS "AWO") and possible GH distribution for northern latitudes from 45° to 90°. In their study (Bogoyavlensky VI et al., 2018a), the authors used the software CSMHYD (Sloan ED et al., 1987; Mehta AP and Sloan ED, 1996) based on the empirical equations of GH stability. The basic data for calculations in CSMHYD were as follows: near-bottom water temperature (World Ocean Database 2013, National Centers for Environmental Information, https://www.ncei.noaa.gov); water mineralization in shallow sediments (two models with salinities of 34.5 psu and 0 psu are considered); and content of hydrate was 100% methane. In these calculations, they also used an array of sea depths available at GEBCO (http://www.gebco.net).

This study aimed to elucidate spatial and intra-annual patterns of distribution of parameters at the upper GHSZ boundary (water temperature, salinity, depth of the upper boundary) based on the oceanographic information for the Sea of Okhotsk for the period from 1929 to 2020.

2. Materials and methods

The upper GHSZ boundary is determined by the intersection of the equilibrium curve of GH dissociation (which depends on thermobaric conditions, gas composition and salinity) with the water temperature distribution curve (Trofimuk AA et al., 1973; Makogon YF, 2003, 2010; Vorobiov AE and Malyukov VP, 2009; Bogoyavlensky VI et al., 2018a, b). Information about the gas composition of hydrates is usually scarce. Based on the materials from expeditions of the VI Il'ichev Pacific Oceanological Institute, Far Eastern Branch, Russian Academy of Sciences (POI FEB RAS), in the Sea of Okhotsk, as well as relevant publications (Veselov OV et al., 2006; Obzhirov AI and Shakirov RB, 2012, 2013; Jin YK et al., 2013, 2015; Shoji H et al., 2014; Minami H et al., 2016; Obzhirov AI, 2018). This study hypothesized that the major component of GHs is "pure" (100%) methane.

For determining the thermobaric conditions of GH stability at the upper GHSZ boundary (with known values of temperature and pressure), one usually uses empirical relationships (Trofimuk AA et al., 1973; Istomin VA and Yakushev VS, 1992; Makogon YF, 2003, 2010; Bogoyavlensky VI et al., 2018b) presented for the "pure

methane–pure (fresh) water" system. Nevertheless, Dickens GR and Quinby-Hunt MS (1994) experimentally determined the conditions of methane hydrate stability for the "pure methane–seawater" system. They showed that the upper GHSZ boundary in seawater should be deeper than in fresh water. Bogoyavlensky VI and co-authors (2018b) drew a similar conclusion: using the model of Sloan ED (1998), they presented the hydrate formation conditions taking into account water salinity. Thus, the higher the water temperature, the greater the difference of the depths required for GH stability in fresh and saline water. For example, at a temperature of 0°C, this difference is 49 m (S = 36.0 psu); at a temperature of +10°C, 120 m (S = 36.0 psu) (Bogoyavlensky VI et al., 2018b). According to our calculations, at a temperature of +1°C (S = 33.5 psu) the depth difference for fresh and saline water should be about 45 m.

This paper calculated the upper GHSZ boundary using the conditions of GH stability obtained by Dickens GR and Quinby-Hunt MS (1994) for the "pure methane–seawater" system (100% methane; salinity 33.5 psu). An example of calculation of the upper GHSZ boundary depth is shown in Fig. 1.

To calculate the upper GHSZ boundary, this study used all available data from deep-sea oceanographic observations in the Sea of Okhotsk. The major part of the data was taken from historical oceanographic arrays provided by RIHMI-WDC (http://meteo.ru), TINRO (http://www.tinro.vniro.ru), and FERHRI (http://ferhri.org). Then, it was extended by the addition of available observation materials from several data centers (National Centers for Environmental Information, https://www.ncei.noaa.gov), and POI FEB RAS (http://www.poi.dvo.ru).

The generalized array of deep-sea observations included bathymetric data (bottle data, OSD), CTD-profiling, and data from drifting "ARGO" buoys. Bathythermographic observations (Mechanical Bathythermograph Data, MBT) and observations with detachable bathythermographs (Expendable Bathythermograph Data, XBT) were also used. The latter two types of observations provide only water temperature profiles.

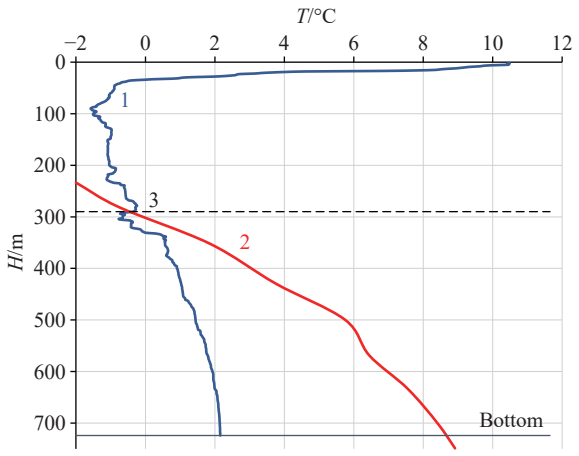

Fig. 1. Diagram of methane hydrate stability (100% CH_4) in seawater: 1–water temperature profile; 2–conditions for methane hydrate stability (S = 33.5 psu) (after Dickens GR and Quinby-Hunt MS, 1994); 3–upper GHSZ boundary (point of curves' intersection).

First, this study carried out a procedure of elimination of duplicate stations, which inevitably occur when an extensive array of observation materials taken from various sources is generalized. Then, using the Ocean Data View software (http://odv.awi.de, 2023), we removed unreliable values (taking into account the regional features of the thermohaline regime of the Sea of Okhotsk).

Afterwards, this paper made interpolation of water temperature and salinity values to the horizons multiple of 5 m at each oceanographic station. Linear interpolation of values was used for processing the bathometric and bathythermographic observations. The CTD observations, data from drifting "ARGO" buoys, and from XBT were re-calculated for the horizons multiple of 5 m using a median procedure (with involving above and below temperature values at a distance of 2.5 m from the calculated one).

After eliminating the duplicate stations and unreliable information, a total of 131286 stations remaining in the resulting oceanographic array for the Sea of Okhotsk were obtained that were performed from 1929 to 2020. Their distribution over the sea is shown in Fig. 2a.

From the presented figure can be seen, that the entire area of the Sea of Okhotsk is sufficiently covered by observations. Nevertheless, an analysis of the database has shown very few oceanographic stations in the cold season in this water area (Fig. 3). This is especially applies to the shelf zone which is covered by sea ice in the cold period of the year. As a result, almost no data is available for this part of the Sea of Okhotsk from January to April.

It should be noted here that the calculation of the upper GHSZ boundary depth was performed for all 131286 stations using the GH stability conditions obtained for the "pure methane–seawater" system (Dickens GR and Quinby-Hunt MS, 1994). As the calculations showed, at the vast majority of stations (99105) in shallow areas of the Sea of Okhotsk, the upper GHSZ boundary in the water column was not determined. The vertical temperature distributions at these oceanographic stations (in the water column), as well as the near-bottom pressure values, indicated that there were no relevant conditions for the GH emergence and stable existence in the water of this shallow part of the sea. This array of stations included also observations in the deep-sea part, where measurements were made only in the upper sea layer due to instrument limitations (e.g., the MBT data array), as well as data from stations with partially rejected information.

The required conditions (water pressure and temperature) for the GH formation and stable state were found only at 32181 stations (24.5% of all oceanographic stations of the compiled data array). Their positions are shown in Fig. 2b. Based on the geographical location of the peripheral stations in this data array, the outer limit of the GHSZ distribution in the water column of the sea are determined.

According to the method presented in the study by Dickens GR and Quinby-Hunt MS (1994) and its graphical

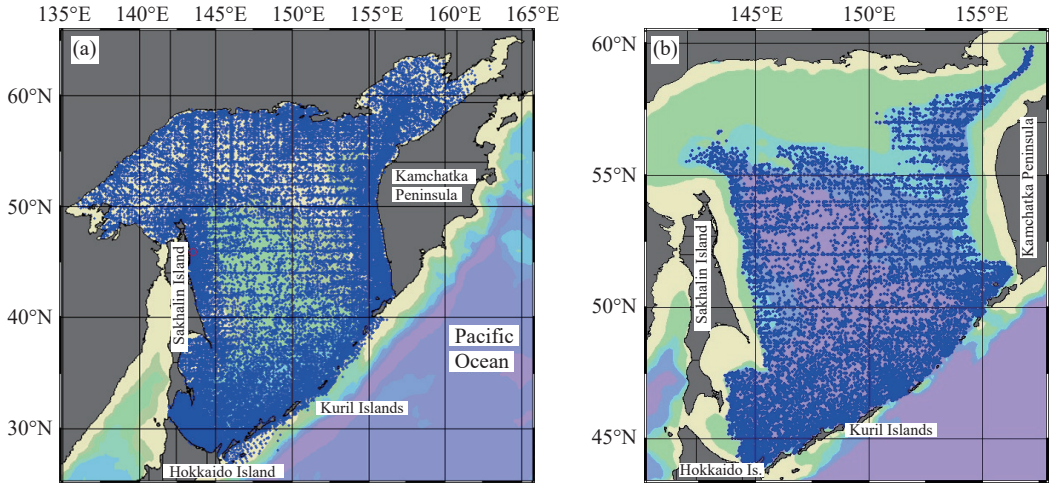

Fig. 2. Spatial distribution of oceanographic stations in the Sea of Okhotsk: a–throughout the period of observations; b–stations where the upper GHSZ boundary was determined.

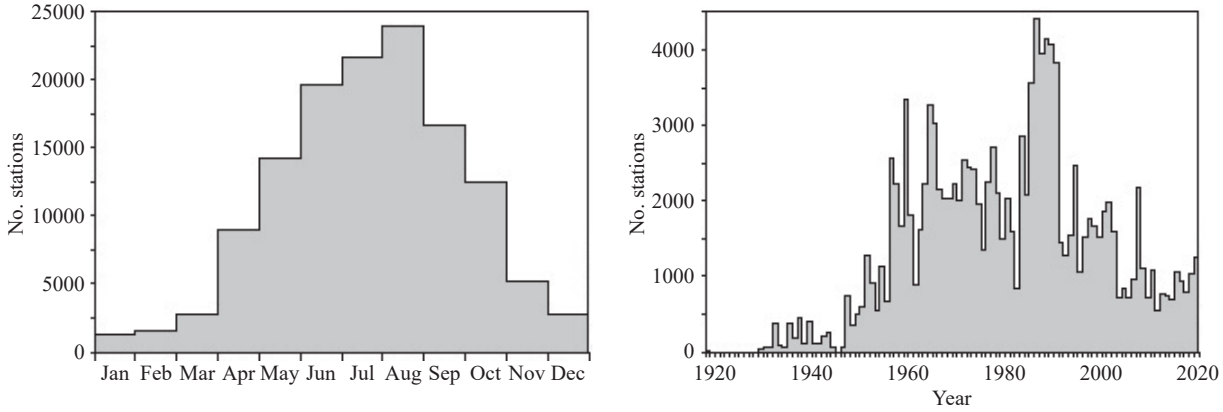

Fig. 3. Temporal distribution of original data.

interpretation (see Fig. 1), the top depth of the GHSZ was determined at each of the 32181 stations. Then a specialized data array was formed, where, in addition to ID information for each station (cruise no., station no., its geographical coordinates, date, and time), the values of the upper GHSZ boundary depth along with the water temperature and salinity at this horizon are input. Additionally, the depth values at each oceanographical station from the GEBCO (http://www.gebco.net) are selected (using coordinates). This data, as well as data of the difference between the depth at each station and the value of the upper GHSZ boundary depth, were entered into a specialized data array that characterized all the obtained parameters at the upper GHSZ boundary.

Average long-term meanings of all the parameters at the upper GHSZ boundary within trapezoids 0.35°×0.55° bounded by longitude and latitude lines are calculated, respectively. To obtain more reliable statistics and smooth out the calculation results, this paper increased the trapezoid dimensions 2.4-fold (while maintaining the step of the calculated grid of 0.35°×0.55°). In each trapezoid, median averaging of initial data is applied. It should also be noted that, when calculating the average long-term statistical parameters in all trapezoids (for normalize the contribution of daily stations, multi-serial stations, and duplicated values), the following operation was performed: Initially, in each trapezoid, all data for a certain day were averaged. The obtained averages per day were assumed to have a unit contribution in further calculations of climatic parameters.

3. Results and discussion

The oceanographic regime of the Sea of Okhotsk, which determines patterns of distribution of the parameters at the GHSZ upper boundary (depth, water temperature, and salinity, and the depth difference between the upper boundary and the seafloor), largely depends on the geographical location, seafloor topography, system of currents in the Sea of Okhotsk (Moroshkin KV, 1966; Kitani K, 1973; Alfultis MA and Martin S, 1987; Gladyshev S et al., 2003; Itoh M et al., 2003; Shcherbina AY et al., 2003; Luchin VA, 2007; Figurkin AL, 2011; Luchin VA and Kruts AA, 2016; Fayman PA et al., 2021), and the morphometry of the straits that connect this sea with the Pacific Ocean and the Sea of Japan (Moroshkin KV, 1966; Kitani K, 1973; Luchin VA, 2007; Luchin VA and Kruts AA, 2016; Fayman PA et al., 2021). The important factors responsible for the formation of certain sea regime are also the dynamics of atmospheric processes above the sea and

the balance of surface heat, especially in the autumn and winter seasons (Kitani K, 1973; Alfultis MA and Martin S, 1987; Martin S et al., 1998; Gladyshev S et al., 2003; Itoh M et al., 2003; Shcherbina AY et al., 2003; Luchin VA, 2007; Figurkin AL, 2011; Luchin VA and Kruts AA, 2016).

The results of our calculations of the parameters at the upper GHSZ boundary have shown as follows. All maps of average long-term monthly data have an invariable basic pattern of spatial distribution. It has been found that in the Sea of Okhotsk waters, the minimum temperature and depth of the upper GHSZ boundary (lower than 1°C and 300–320 m, respectively) in all the maps occur off the eastern slope of Sakhalin Island and in the southwestern part of the sea. However, the maximum temperature and depth of the GHSZ upper boundary (1.5°C–2.0°C and 340–360 m, respectively) for all months are typical of the waters adjacent to the central and northern straits of the Kuril Islands.

To identify the characteristic months that would reflect possible extreme features in the spatial distributions of the calculated parameters at the GHSZ upper boundary, consider the known results highlighting the patterns of seasonal variations in oceanographic conditions in the active layer of the Sea of Okhotsk waters. In the study by Luchin VA (2007), the active layer of the sea was identified taking into account statistically significant intra-annual variations in water temperature. As the author assumed, if the range of seasonal temperature variations on a specified horizon was greater than the sum of errors for the months with extreme values, then it was considered reliable. The calculations showed that statistically significant seasonal temperature variations in Sea of Okhotsk waters are usually observed to depth horizons from 75 m to 500–600 m. A map of the lower limit of the active layer in the Sea of Okhotsk (Luchin VA, 2007), modified to meet the objectives of the present study, is provided in Fig. In particular, this figure shows an area of the sea where thermobaric conditions make the formation and presence of GHs in seawater impossible.

As follows from the figure presented, seasonal variations in water temperature can be observed in dynamically active areas of the sea (such as the Kuril straits and the TINRO Basin) to maximum depths (from 300 m to 500–600 m). It is known (Kitani K, 1973; Martin S et al., 1998; Gladyshev S et al., 2003; Itoh M et al., 2003; Figurkin AL, 2011; Luchin VA and Kruts AA, 2016) that the annual pattern of variations in water temperature at subsurface horizons is a result of differentiated contribution of weather conditions, the wind- and wave-induced mixing of the upper water layer, and the transformation of waters in dynamically active regions. As a rule, the range of intra-annual fluctuations in water temperature reduces significantly with depth. Moreover, in waters remote from dynamically active zones, seasonal variations in water temperature are distinguished with confidence only in a thin surface layer (0–30 m). Thus, with increasing depth, there is a time lag for the onset of maximum and minimum water temperature values from horizon to horizon. In dynamically active areas of the sea, a distinct seasonal variation in water temperature is observed in the layer 0–75 m. Here, the range of seasonal water temperature variations is minimum. Moreover, the shift in the onset of maximum/minimum water temperature values from horizon to horizon is also manifested to a lesser extent here. The geographical location and configuration of areas with increased values of seasonal water temperature variations at the subsurface horizons also agree well with the existing cyclonic system of non-periodic sea currents (Moroshkin KV, 1966; Luchin VA, 1982, 1987; Fayman PA et al., 2021).

Thus, a comparative analysis of our calculations of the parameters at the upper GHSZ boundary with the data in Fig. 4 allows us to conclude that, over the major part of the Sea of Okhotsk, the upper GHSZ boundary is located much deeper than the lower limit of the active layer. The only exception is the zone near the Kuril Islands and the area of the TINRO Basin.

For these water areas, the average long-term monthly data of position of the upper GHSZ boundary and the respective water temperature are considered. It has been found (based on the patterns of seasonal variations of these parameters within three 2-degree trapezoids located west of the Kuril Islands and within one trapezoid in the area of the TINRO Basin) that the minimum values of the parameters under consideration in these areas occur in May and June, and the maximum in November and December. Therefore, for further analysis of the patterns of spatial distribution of the parameters at the upper GHSZ boundary, maps only for the months with extreme values during the annual cycle (respectively, average distributions for May–June and November–December) were composed.

Fig. 5 shows the spatial distribution of the average long-term water temperature values at the upper GHSZ boundary for May–June and November–December. Their major and distinctive feature is the invariability of the main large-scale pattern of distribution of water temperatures in the months with extreme intra-annual values (with maximum values at the central Kuril straits and minimum values off the western

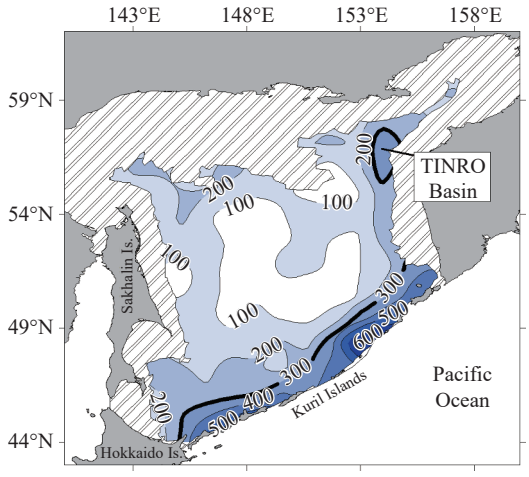

Fig. 4. Lower limit (m) of the active layer of the Sea of Okhotsk waters (the shaded area indicates a zone that lacks thermobaric conditions for GHs to form and exist in the water column).

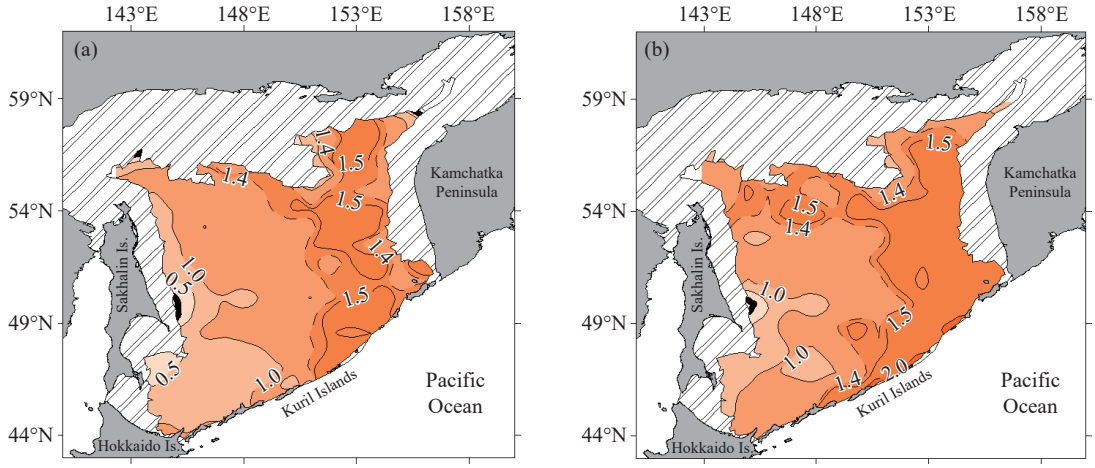

Fig. 5. Spatial distribution of average long-term water temperature values (°C) in the Sea of Okhotsk at the upper GHSZ boundary: a–in May–June; b–in November–December (isotherm 0°C is drawn as solid line; the shaded area indicates a zone that lacks thermobaric conditions for GHs to form and exist in the water column).

slope of the deep-sea basin).

In general, intra-annual temperature variations are poorly detected at the depth of the upper GHSZ boundary, except for dynamically active water area (near the Kuril straits and in the areas near the deep-sea basin slopes). On the basis of temperature values at the upper GHSZ boundary, the sea be divided into two parts, with the border between them being the isotherms 1.4°C and 1.5°C (Fig. 5).

In the eastern, relatively warm, sector of the sea, the maximum water temperature values are recorded from the Kuril straits and the adjacent waters of the Sea of Okhotsk. Here, this occurs due to the intense tidal mixing in the straits, as a result of which the heat is transferred to the horizons of the upper GHSZ boundary from the horizons above and below. In the southernmost part of the sea, there is also a zone with elevated water temperatures (which becomes more evidently pronounced in November and December), associated with the mixing of the Sea of Okhotsk cold waters and the warmer water of the Soya Current. It should also be noted that the differences in temperature values from May–June to November–December are recorded with confidence from both sectors of the sea (the differences amount to about 0.5°C in the cold sector of the sea and slightly less in the warm one).

The spatial distributions of water temperatures at the upper GHSZ boundary well agree also with the cyclonic system of the sea currents described in other studies (Moroshkin KV, 1966; Luchin VA, 1982, 1987; Fayman PA et al., 2021). As a result, an area of elevated water temperature is observed over the continental slope of the eastern and northern parts of the sea (see the position of isotherms 1.4°C and 1.5°C). The effect of movement and gradual transformation of Pacific water in the Sea of Okhotsk becomes most evidently pronounced in November–December (Fig. 5). Moreover, the presented maps clearly show a decrease in water temperature as the Pacific water is spread and transformed in the sea (over the southern deep-sea basin and west of the Kamchatka Peninsula), which is a consequence of their mixing with the supercooled waters of the Sea of Okhotsk.

In the cold sector of the sea, an area with the lowest temperature values at the upper GHSZ boundary is distinguished in the westernmost part of the sea. In the north, this water area is bounded by a canyon located south of Iony Island and Kashevarov Bank; in the south, by the slope of the Gulf of Terpenya. This area is formed through two major processes. First, it is the autumn–winter convection and ice formation on the northern shelf of the sea. This dense and supercooled shelf water forms in winter in coastal areas of the northwestern Sea of Okhotsk and has the lowest temperature in the sea (Kitani K, 1973; Alfultis MA and Martin S, 1987; Talley LD, 1991; Martin S et al., 1998; Wong CS et al., 1998; Gladyshev S et al., 2003; Shcherbina AY et al., 2003). Then, it moves to the continental slope area with the cyclonic system of sea currents. An additional effect during the formation of the area with low water temperature in the westernmost part of the study region is exerted by the intensification of tidal and non-periodic currents over the continental slope of the sea and also in the shallow waters near Iony Island and Kashevarov Bank. It should also be noted that the lowest temperature values (lower than 0.5°C) in the cold sector of the Sea of Okhotsk become more pronounced in May–June. According to the configuration of isotherm 1°C (especially in May–June), the supercooled water moves south (to the latitude of Cape Aniva) and then east (with the cyclonic system of currents in the sea).

A distinctive feature of the salinity fields at the upper GHSZ boundary (in May–June and November–December) is the invariability of the general patterns of the spatial salinity distribution. As follows from the maps in Fig. 6, the salinity values at the upper GHSZ boundary in the Sea of Okhotsk vary within a rather narrow range (from 33.3 to 33.7 psu). Moreover, in most of the study area and throughout the year, the salinity values are not higher than 33.4–33.6 psu, which is quite close to the conditions for the MH stability in seawater, according to Dickens GR and Quinby-Hunt MS (1994).

In May and June, minimum salinity values at the upper GHSZ boundary are usually recorded from the peripheral

areas of the Sea of Okhotsk (Fig. 6a). The only exception is the waters adjacent to the central and northern straits of the Kuril Islands (the major inflow of Pacific water into the sea).

The most extensive area with low salinity (and low water temperature) is observed off the Sakhalin Island slope (Figs. 5, 6). As is known (Kitani K, 1973; Alfultis MA and Martin S, 1987; Talley LD, 1991; Martin S et al., 1998; Wong CS et al., 1998; Gladyshev S et al., 2003; Shcherbina AY et al., 2003), here the formation of the salinity field is dominated by the near-bottom shelf waters in the northwestern part of the sea (with a low temperature and salinity) that are formed through the autumn–winter convection. This stationary area with decreased salinity values east of Sakhalin also depends on the advection of relatively fresh water whose regime is strongly dependent on the Amur River discharge (waters northeast of Sakhalin Gulf and east of Sakhalin Island).

As follows from the configuration of the area with salinities below 33.5 psu (Fig. 6a), upon reaching the southern part of the sea, this freshened water, first, enters the Pacific Ocean, which contributes to the formation of an intermediate water mass with decreased salinity in its northwestern part (Talley LD, 1991; Yasuda I, 1997; Shcherbina AY et al., 2003; Ono K et al., 2007; Ohshima KI et al., 2010). Moreover, the currents of the southern periphery of the cyclonic gyre (over the central part of the sea) move these freshened waters eastward to the longitude of the central Kuril straits. In autumn and early winter (see Fig. 6b), the area of freshened waters reaches the western slope of the Kamchatka Peninsula.

The maximum salinity values at the upper GHSZ boundary are recorded from two areas of the sea. The first is a local area in the southern part of the Kuril Basin (offshore of the Shiretoko Peninsula, Hokkaido Island), especially pronounced in November and December. Increased salinity values in this region are formed through the interaction and vertical mixing of Pacific water, Soya current water, and Sea of Okhotsk water proper (Gladyshev S et al., 2003; Itoh M et al., 2003), which causes temperature and salinity to increase here (Fig. 5, 6).

The second area with increased salinity values is located near the central and northern Kuril straits, where highly saline water from the Pacific Ocean enters the sea (Fig. 6). This formed anomaly of increased salinity expands all over the central and northeastern Sea of Okhotsk.

In the central part of the sea (north of the 49° N), the process of filling the areas near the slope with the transformed Pacific water (with higher salinity) is clearly manifested (when considering the configuration and size of areas with salinities higher than 33.5 psu) from May–June to November–December. As a result (due to the advection of the modified Pacific water in the system of sea currents), waters with low salinity values at the upper GHSZ boundary disappear from the areas near the slope of northeastern Sakhalin and Kamchatka in November–December.

The GHSZ top depth in the Sea of Okhotsk (Fig. 7) is fully consistent with the above-discussed oceanographic conditions (Figs. 5, 6) and the above-indicated main factors of their formation (the autumn–winter convection, the lateral and vertical mixing at boundaries of currents and in the Kuril straits, the advections of Pacific water and Sea of Japan water, and the intensification of tidal and non-periodic currents in areas of sharp depth variations).

As follows from Fig. 7, the GHSZ top depth in the Sea of Okhotsk varies from 300 m to 360 m. A maximum depth (up to 340–360 m) is observed near the central and northern Kuril Islands (the main inflow of warm Pacific water to the Sea of Okhotsk). The upper GHSZ boundary closest to the sea surface is located off the Sakhalin Island continental slope (Fig. 7). In spring, the area of minimum depth of the upper GHSZ boundary (shallower than 320–330 m) becomes most pronounced and spreads over the continental slope (from the northern tip of Sakhalin Island to Hokkaido, Fig. 7a). Moreover, the topography of the upper GHSZ boundary in the western part of the sea (with depths to 320 m and 330 m, Fig. 7) agrees well with the cyclonic system of currents in the Sea of Okhotsk.

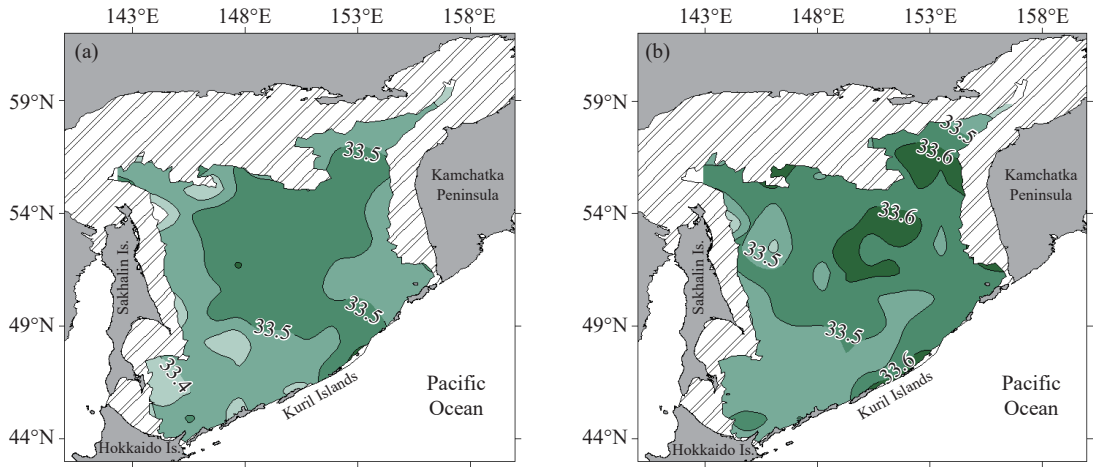

Fig. 6. Spatial distribution of average long-term water salinity values (psu) in the Sea of Okhotsk at the upper GHSZ boundary: a–in May–June; b–in November–December (the shaded area indicates a zone that lacks thermobaric conditions for GHs to form and exist in the water column).

Fig. 8 shows the spatial distribution of the average long-term difference of depths between the upper GHSZ boundary and the seafloor. It should be noted that over the major part of the Sea of Okhotsk, an almost invariable distribution of depth differences is observed from May–June to November–December. This is explained mainly by small spatial variations in the depth of the upper GHSZ boundary (Fig. 7), as well as by great spatial variations in the seafloor topography of the Sea of Okhotsk. Small differences are observed only in the sectors of the continental slope in the central and northern Sea of Okhotsk (north of 49° N). The latter is related, first, with the minimum distances between the upper GHSZ boundary and the seafloor (Fig. 8). Moreover, maximum intra-annual water temperature and salinity variations are recorded from these areas of the northern part of the sea (Figs. 5, 6).

It is also worth noting here that the division of the water area of the Sea of Okhotsk into conditions favorable/unfavorable for GH formation and existence that made in this paper (in all the maps, Figs. 5–9) is consistent with the data provided in a number of relevant studies (Ginsburg GD et al., 1990; Bogoyavlensky VI et al., 2018a). Nevertheless, the division of the sea area shown in Figs. 5–9 is more detailed, while the differences from the data in the above-mentioned studies (Ginsburg GD et al., 1990; Bogoyavlensky VI et al., 2018a) are mainly explained by the use of a more complete array of original oceanographic data in the present study, with the actual thermal structure of Sea of Okhotsk waters taken into account in calculations and with a more realistic assumption as regards the GH stability condition for the "pure methane–seawater" system (S = 33.5 psu).

In the present study, the probability of existence of cryogenic GHs (although negative temperature values exist over the major part of the Sea of Okhotsk shelf) is not considered. First, this issue is beyond the scope of our study (sea water column). Second, an explanation for the probability of existence of cryogenic GHs and their presumed localization within the Sea of Okhotsk was described in enough detail by Bogoyavlensky VI et al. (2018a).

Reliability of the results that obtained in this study is estimated on the basis of localization of the identified GH deposits and methane plumes (seeps). This data was obtained

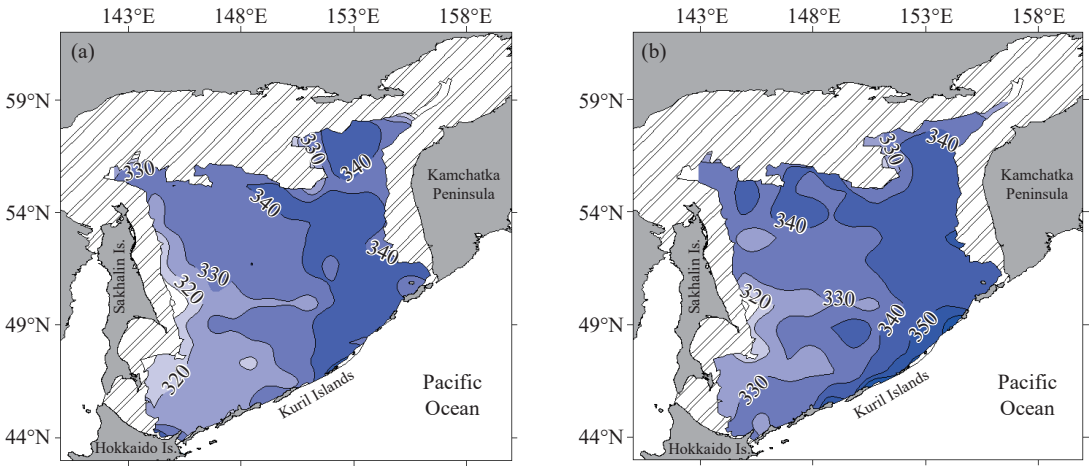

Fig. 7. Spatial distribution of average long-term values of the upper GHSZ boundary depth (m) in the Sea of Okhotsk: a–in May–June; b–in November–December (the shaded area indicates a zone that lacks thermobaric conditions for GHs to form and exist in the water column).

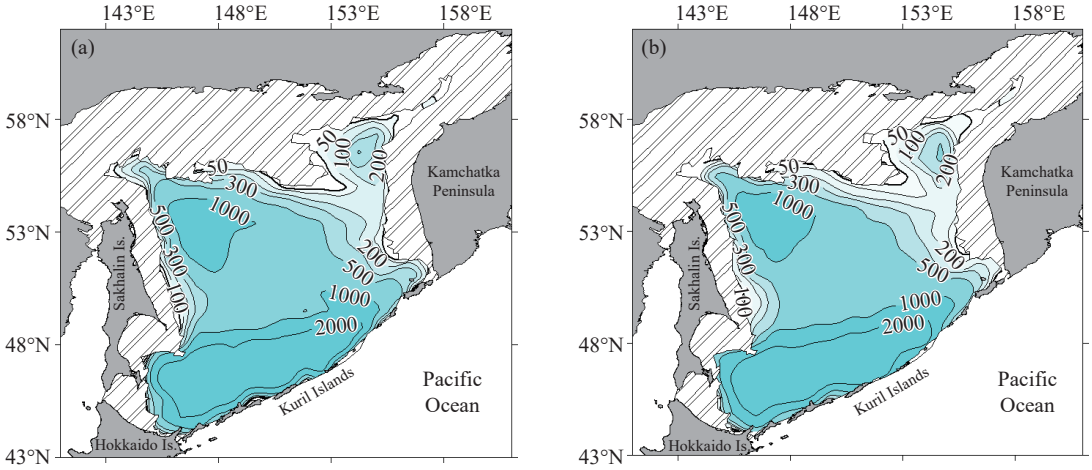

Fig. 8. Spatial distribution of average long-term values of depth difference (m) between the upper GHSZ boundary and the seafloor in the Sea of Okhotsk: a–in May–June; b–in November–December (the shaded area indicates a zone that does not meet the thermobaric conditions for hydrate formation).

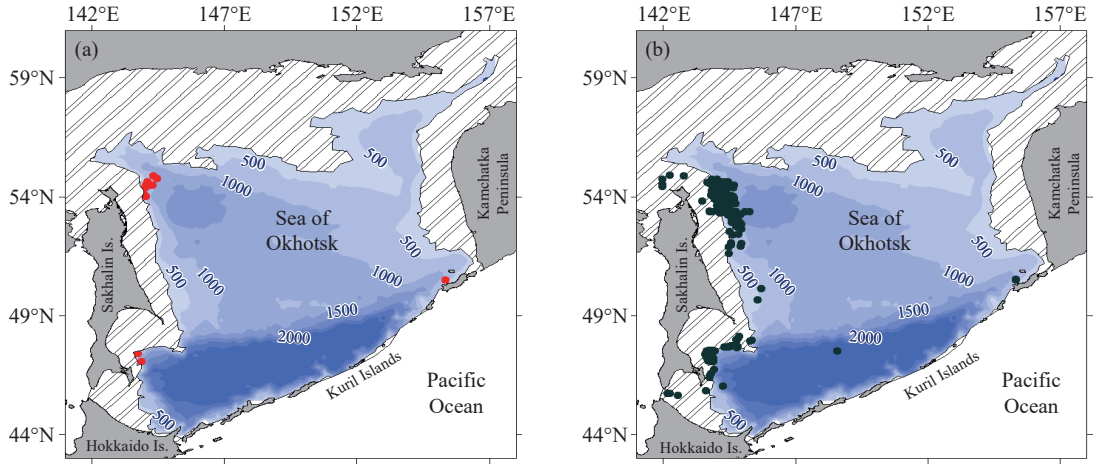

Fig. 9. Bathymetric map of the Sea of Okhotsk (main isobaths are indicated by numerals) showing the known GH accumulations confirmed by direct methods (a) and methane seeps (b) (the shaded area indicates a zone that lacks thermobaric conditions for GHs to form and exist in the water column).

within the framework of long-term observations during the POI FEB RAS expeditions for the period 1988–2021 and published in part (Obzhirov AI and Shakirov RB, 2012, 2013; Jin YK et al., 2013, 2015; Shoji H et al., 2014; Minami H et al., 2016; Obzhirov AI, 2018). As follows from Fig. 9a, the GH deposits detected by the contact methods are located in and tend to the water area where the upper GHSZ boundary runs in the water column. The pattern of distribution of the identified methane plumes in the Sea of Okhotsk waters is more complex but comprehensible (Fig. 9b). These are distributed not only in the zone with the lack of thermobaric conditions for GH formation and existence in the water column but also in the deep-sea part.

The existence of methane plumes in the shallow parts of the study area is associated, first, with the oil and gas deposits and active faults in the sediment layer. Here, in the water column also (and probably in the upper sediment layer), there are no thermobaric conditions for the formation and existence of GHs that can act, by "cementing" bottom sediments, as a fluid-impermeable seal. Second, in these areas of the sea, the upper GHSZ boundary can run both near the seafloor and in the upper part of the sediment layer. Therefore, thermal conditions favorable for GH dissociation can form here. This can be evidenced by the well-known facts of both seasonal and year-to-year fluctuations in water temperature in the Sea of Okhotsk (Gladyshev S et al., 2003; Itoh M et al., 2003; Shcherbina AY et al., 2003; Luchin VA and Zhigalov IA, 2006; Luchin VA, 2007; Nakanowatari T et al., 2007; Ohshima KI et al., 2010; Figurkin AL, 2011).

The presence of methane seeps in the deep-sea part (Fig. 9b), where thermobaric conditions in the water column are favorable for GH formation and existence, can be explained by effects of the following factors. Here, disturbances in the structure of host sediments may occur due to seismic and tectonic processes (especially in fault zones), which may also cause gas emissions. As is known, episodes of seismic and volcanic/magmatic activity are currently observed in the Sea of Okhotsk region. Another factor is apparently some additional sources in the form of accumulations of hydrocarbons, foci of post-magmatic processes, etc., which will be considerd in subsequent publications.

4. Conclusions

Based on an extensive oceanographic data base for the Sea of Okhotsk for the period from 1929 to 2020 and the use of the GH stability conditions (Dickens GR and Quinby-Hunt MS, 1994) for the "pure methane–seawater" system, the spatiotemporal patterns of distribution of parameters at the upper GHSZ boundary such as water temperature, salinity, and GHSZ top depth are identified.

The data for the extreme periods in the annual variations (May–June and November–December) has shown invariability of the major patterns of average long-term spatial distribution of these parameters at the upper GHSZ boundary in the Sea of Okhotsk. The Minimum values of the temperature and GHSZ top depth (less than 1°C and 300–320 m, respectively) to occur off the eastern slope of Sakhalin Island is found. Maximum water temperatures and GHSZ top depth (1.5°C–2.0°C and 340–360 m, respectively) have proven to be typical of the southeastern sea area adjacent Kuril Islands.

The presented results are expected be in demand for designing gas hydrates surveys in the Sea of Okhotsk and also for studying the effect that GHs and consequences of their dissociation exert on the distribution of marine microorganisms. Furthermore, the position of the top depth and the extent of GHSZ in the water column are the essential parameters for modeling scenarios of methane hydrates response to temperature variations near the seafloor and for assessing the probability of methane emission into the ecosystem. The patterns that is identified in this study will find application in simulations to study the dynamics of dissolution of rising gas bubbles in the water column.

CRediT authorship contribution statement

The authors made equal contributions at all stages of

preparation of the paper (objective setting, calculations, analysis of results, and writing of text). All authors discussed the results obtained from the study and contributed to the final version of this article.

Declaration of competing interest

The authors declare no conflicts of interest.

Acknowledgments

The authors express their sincere gratitude to the reviewers for the constructive comments. This study is a contribution to fulfilling the goals of the GEOMIR project within the framework of the national action plan for the United Nations Decade of Ocean Sciences for Sustainable Development (2021–2030) and the WESTPAC Working Group on Gas Hydrates and Methane Fluxes in the Indo-Pacific Region. The study was carried out in accordance with the state budget topic for the POI FEB RAS, entitled “Study of the Structure and Dynamics of World’s Oceans Waters in Conditions of Current Climate Change” (reg. no. 124022100079-4).

References

Alfultis MA, Martin S. 1987. Satellite passive microwave studies of the Sea of Okhotsk ice cover and its relation to oceanic processes, 1978–1982. Journal of Geophysical Research: Oceans, 92(C12), 13013–13028. doi: 10.1029/jc092ic12p13013.

Biastoch A, Treude T, Rüpke LH, Riebesell U, Roth C, Burwicz EB, Park W, Latif M, Böning CW, Madec G, Wallmann K. 2011. Rising Arctic Ocean temperatures cause gas hydrate destabilization and ocean acidification. Geophysical Research Letters, 38(8), L08602. doi: 10.1029/2011gl047222.

Bogoyavlensky V, Kishankov A, Yanchevskaya A, Bogoyavlensky I. 2018a. Forecast of gas hydrates distribution zones in the Arctic Ocean and adjacent offshore areas. Geosciences, 8(12), 453. doi: 10.3390/geosciences8120453.

Bogoyavlensky VI, Yanchevskaya AS, Bogoyavlensky IV, Kishankov AV. 2018b. Gas hydrates in the Circum-Arctic Region aquatories. Arctic: Ecology and Economy, 3(31), 42–55 (in Russian with English abstract). doi: 10.25283/2223-4594-2018-3-42-55.

Chen ZA, Bai WM, Xu WY. 2005. Prediction of stability zones and occurrence zones of Multiple composition natural gas hydrate in marine sediment. Chinese Journal of Geophysics, 48(4), 939–945. doi: 10.1002/cjg2.733.

Chen ZA, Bai WM, Xu WY, Jin ZH. 2010. An analysis on stability and deposition zones of natural gas hydrate in Dongsha Region, north of South China Sea. Journal of Thermodynamics, 185639. doi: 10.1155/2010/185639.

Dickens GR, Quinby-Hunt MS. 1994. Methane hydrate stability in seawater. Geophysical Research Letters, 21(19), 2115–2118. doi: 10.1029/94gl01858.

Eliseev AV. 2018. Global methane cycle: A review. Fundamental and Applied Climatology, 1, 52–70. doi: 10.21513/2410-8758-2018-1-52-70.

Fayman PA, Prants SV, Budyansky MV, Uleysky MY. 2021. Simulated pathways of the northwestern Pacific water in the Okhotsk Sea. Izvestiya, Atmospheric and Oceanic Physics, 57(3), 329–340. doi: 10.1134/s000143382103004x.

Figurkin AL. 2011. Variability of temperature and salinity from bottom waters in the northern Okhotsk Sea. Izvestiya TINRO, 166, 255–274 (in Russian with English abstract).

Ginsburg GD, Gramberg IS, Soloviev VA. 1990. Geology of submarine gas hydrates. Sovietskaya Geologiya, 11, 12–19 (in Russian).

Giustiniani M, Tinivella U, Jakobsson M, Rebesco M. 2013. Arctic ocean gas hydrate stability in a changing climate. Journal of Geological Research, 783969. doi: 10.1155/2013/783969.

Gladyshev S, Talley L, Kantakov G, Khen G, Wakatsuchi M. 2003. Distribution, formation, and seasonal variability of Okhotsk Sea mode water. Journal of Geophysical Research: Oceans, 108(C6), 3186. doi: 10.1029/2001jc000877.

Granin NG, Makarov MM, Kucher KM, Gnatovsky RY. 2010. Gas seeps in Lake Baikal-detection, distribution, and implications for water column mixing. Geo-Marine Letters, 30(3–4), 399–409. doi: 10.1007/s00367-010-0201-3.

Holder GD, Malone RD, Lawson WF. 1987. Effects of gas composition and geothermal properties on the thickness and depth of natural-gas-hydrate zones. Journal of Petroleum Technology, 39(9), 1147–1152. doi: 10.2118/13595-pa.

Istomin VA, Yakushev VS. 1992. Gas hydrates in natural conditions. Nedra, Moscow, 236 (in Russian).

Itoh M, Ohshima KI, Wakatsuchi M. 2003. Distribution and formation of Okhotsk Sea intermediate water: An analysis of isopycnal climatological data. Journal of Geophysical Research: Oceans, 108(C8), 3258. doi: 10.1029/2002jc001590.

Jin YK, Shoji H, Obzhirov A, Baranov B. 2013. Operation report of Sakhalin slope gas hydrate project 2012, R/V Akademik MA Lavrentyev, Cruise 59. Korea Polar Research Institute, 163.

Jin YK, Minami H, Baranov B, Nikolaeva N, Obzhirov A. 2015. Operation Report of Sakhalin Slope Gas Hydrate Project II, 2014, R/V Akademik MA Lavrentyev, Cruise 67. Korea Polar Research Institute, 121.

Kitani K. 1973. An oceanographic study of the Okhotsk Sea-particularly in regard to cold waters. Bull. Far Seas Fisheries Research Laboratory, 9, 45–77.

Luchin VA. 1982. Diagnostic calculation of water circulation in the Sea of Okhotsk in a summer season. Trudy DVNIGMI, 96, 69–77 (in Russian).

Luchin VA. 1987. The Sea of Okhotsk circulation and features of its interannual variability as referred from diagnostic calculations, Trudy DVNIGMI, 36, 3–13 (in Russian).

Luchin VA. 2007. Seasonal variations in water temperature in the active layer of Far East Seas, in Dal'nevostochnye morya Rossii (Far East Seas of Russia), Book 1, Nauka, Moscow, 232–252 (in Russian).

Luchin VA, Zhigalov IA. 2006. Types of water temperature distribution in active layer of the Okhotsk Sea and possibility of its prediction. Izvestiya TINRO, 147, 183–204 (in Russian with English abstract).

Luchin VA, Kruts AA. 2016. Properties of cores of the water masses in the Okhotsk Sea. Izvestiya TINRO, 184(1), 204–218. doi: 10.26428/1606-9919-2016-184-204-218.

Makogon YF. 2003. Natural gas hydrates: Distribution, models of formation, resources. Russian Chemistry Journal, 47(3), 70–79 (in Russian).

Makogon YF. 2010. Gas hydrates, History of development and prospects of study. Geology and mineral resources of World Ocean, 2, 5–21 (in Russian).

Martin S, Drucker R, Yamashita K. 1998. The production of ice and dense shelf water in the Okhotsk Sea polynyas. Journal of Geophysical Research: Oceans, 103(C12), 27771–27782. doi: 10.1029/98jc02242.

McGinnis DF, Greinert J, Artemov Y, Beaubien SE, Wüest A. 2006. Fate of rising methane bubbles in stratified waters: How much methane reaches the atmosphere? Journal of Geophysical Research:

Oceans, 111(C9), C09007. doi: 10.1029/2005jc003183.
Mehta AP, Sloan ED. 1996. Improved thermodynamic parameters for prediction of structure H hydrate equilibria. AIChE Journal, 42(7), 2036–2046. doi: 10.1002/aic.690420724.
Bondur VG, Mokhov II, Macosko AA. 2022. Methane and climate change: Scientific problems and technological aspects. Russian Academy of Sciences, Moscow, 388 (in Russian).
Minami H, Jin YK, Baranov B, Nikolaeva N, Obzhirov A. 2016. Operation Report of Sakhalin Slope Gas Hydrate Project II, 2015, R/V Akademik MA Lavrentyev, Cruise 70. Kitami Institute of Technology, 119.
Moroshkin KV. 1966. Water masses of the Sea of Okhotsk. Nauka, Moscow, 70 (in Russian).
Nakanowatari T, Ohshima KI, Wakatsuchi M. 2007. Warming and oxygen decrease of intermediate water in the northwestern North Pacific, originating from the Sea of Okhotsk, 1955–2004. Geophysical Research Letters, 34(4), L04602. doi: 10.1029/2006gl028243.
Obzhirov AI. 2018. Gasgeochemical precursors of seismic activity, earthquakes, volcanic episodes on the Kamchatka and Sea of Okhotsk (to use information of the Kamchatka scientific conferences 2017). Geosystems of Transition Zones, 2(1), 57–68 (in Russian with English abstract). doi: 10.30730/2541-8912.2018.2.1.057-068.
Obzhirov AI, Shakirov RB. 2012. Gas hydrate complex geological and geophysical investigation in the Okhotsk Sea. Geology and geoecology of Eurasian continental margins, 4, Special issue, Geology and mineral resources of the Eurasian marginal seas, GEOS, Moscow, 122–136 (in Russian).
Obzhirov AI, Shakirov RB. 2013. Sources of hydrocarbon gases, conditions of gas hydrate formation, and their relation with petroleum reservoirs in the Sea of Okhotsk. Oceanographic studies of the Far Eastern Seas and North-Western Pacific, Book 2, Dalnauka, Vladivostok, 149–161 (in Russian).
Ohshima KI, Nakanowatari T, Riser S, Wakatsuchi M. 2010. Seasonal variation in the in- and outflow of the Okhotsk Sea with the North Pacific. Deep Sea Research Part II: Topical Studies in Oceanography, 57(13–14), 1247–1256. doi: 10.1016/j.dsr2.2009.12.012.
Ono K, Ohshima KI, Kono T, Itoh M, Katsumata K, Volkov YN, Wakatsuchi M. 2007. Water mass exchange and diapycnal mixing at Bussol' Strait revealed by water mass properties. Journal of Oceanography, 63(2), 281–291. doi: 10.1007/s10872-007-0028-3.
Reagan MT, Moridis GJ. 2007. Oceanic gas hydrate instability and dissociation under climate change scenarios. Geophysical Research Letters, 34(22), L22709. doi: 10.1029/2007gl031671.
Reagan MT, Moridis GJ, Elliott SM, Maltrud M. 2011. Contribution of oceanic gas hydrate dissociation to the formation of Arctic Ocean methane plumes. Journal of Geophysical Research, 116(C9), C09014. doi: 10.1029/2011jc007189.
Shcherbina AY, Talley LD, Rudnick DL. 2003. Direct observations of North Pacific ventilation: Brine rejection in the Okhotsk Sea. Science, 302(5652), 1952–1955. doi: 10.1126/science.1088692.
Shoji H, Jin YK, Baranov B, Nikolaeva N, Obzhirov A. 2014. Operation Report of Sakhalin Slope Gas Hydrate Project II, 2013, R/V Akademik MA Lavrentyev, Cruise 62. Environmental and Energy Resources Research Center, Kitami Institute of Technology, Kitami, 111.
Sloan ED. 1998. Off shore hydrate engineering handbook. Center for Hydrate Research, Colorado School of Mines. Golden, Colorado.
Sloan ED, Sparks KA, Johnson JJ. 1987. Two-phase liquid hydrocarbon-hydrate equilibrium for ethane and propane. Industrial & Engineering Chemistry Research, 26(6), 1173–1179. doi: 10.1021/ie00066a019.
Sloan ED, Koh CA. 2008. Clathrate Hydrates of Natural Gases. CRC Press, Boca Raton, Fla, USA, 3rd edition, 752. doi: 10.1201/9781420008494.
Smyshlyaev SP, Mareev EA, Galin VY, Blakitnaya PA. 2015. Modeling the influence of methane emissions from Arctic gas hydrates on regional variations in composition of the lower atmosphere. Izvestiya, Atmospheric and Oceanic Physics, 51(4), 412–422. doi: 10.1134/s000143381504012x.
Talley LD. 1991. An Okhotsk Sea water anomaly: Implications for ventilation in the North Pacific. Deep Sea Research Part A. Oceanographic Research Papers, 38(1), S171–S190. doi: 10.1016/S0198-0149(12)80009-4.
Trofimuk AA, Cherskiy NV, Tsarev VP. 1973. Accumulation of natural gases in zones of hydrate formation in the hydrosphere. Doklady Akademii Nauk SSSR, 212(4), 931–934 (in Russian).
Veselov OV, Gordienko VV, Kudelkin VV. 2006. Thermobaric conditions of gas hydrate formation in the Sea of Okhotsk. Geology and Mineral Resources of World Ocean, 3(5), 62–68 (in Russian).
Vorobiov AE, Malyukov VP. 2009. Gas hydrates. Technologies of influence on unconventional hydrocarbons: Manual, the revised & added 2nd edition, Peoples' friendship Russian University (RUDN), Moscow, 289 (in Russian).
Wong CS, Matear RJ, Freeland HJ, Whitney FA, Bychkov AS. 1998. WOCE line P1W in the Sea of Okhotsk: 2. CFCs and the formation rate of intermediate water. Journal of Geophysical Research: Oceans, 103(C8), 15625–15642. doi: 10.1029/98jc01008.
Yakutseni VP. 2013. Gas hydrates–unconventional gas sources, their formation, properties, distribution and geological resources. Petroleum Geology - Theoretical and Applied Studies, 8(4), 1–24 (in Russian with English abstract).
Yasuda I. 1997. The origin of the North Pacific intermediate water. Journal of Geophysical Research: Oceans, 102(C1), 893–909. doi: 10.1029/96jc02938.